E9632
5-3-95

NASA Technical Memorandum 106920

"Fundamental Concepts" of Integrated and Fiber Optic Sensors

Margaret L. Tuma
Lewis Research Center
Cleveland, Ohio

May 1995

National Aeronautics and
Space Administration

"FUNDAMENTAL CONCEPTS" OF INTEGRATED AND FIBER OPTIC SENSORS

Margaret L. Tuma
National Aeronautics and Space Administration
Lewis Research Center
Cleveland, Ohio 44135

INTRODUCTION

This chapter discusses fiber optic and integrated optic sensor concepts. Unfortunately, there is no standard method to categorize these sensor concepts. Here, fiber optic and integrated optic sensor concepts will be categorized by the primary modulation technique. These modulation techniques have been classified as: intensity, phase, wavelength, polarization, and time/frequency modulation [1],[2],[3],[4]. All modulate the output light with respect to changes in the physical or chemical property to be measured. Each primary modulation technique is then divided into fiber optic and integrated optic sections which are treated independently. For each sensor concept, possible sensor applications are discussed. The sensors and references discussed are not exhaustive, but sufficient to give the reader an overview of sensor concepts developed to date. Sensor multiplexing techniques [5] such as wavelength division, time division, and frequency division will not be discussed as they are beyond the scope of this chapter.

1.1 Intensity Modulation - Sensor Concepts

Intensity-modulated sensors vary the output light intensity with respect to the measurand. This scheme was employed in the earliest optical sensors because of its simplicity, reliability, and low cost. However, intensity-modulated sensors are susceptible to drift caused by source intensity variations, variable losses in fibers and connectors, and sensitivity changes of the detectors [3], [4]. Thus, a referencing technique is needed to avoid signal corruption. Three referencing techniques will be discussed.

Referencing

A simple referencing technique sends part of the source light to the sensor and the rest is used as a reference. Each part is directed to a unique detector. Source output variations can be eliminated by dividing the sensor signal by the reference signal. However, intensity fluctuations due to coupling loss variations and detector drift are not compensated for when using this scheme. To do so requires two distinguishable return channels from the sensor [3], which the next two techniques possess.

The second referencing scheme can be used only if both the fiber loss and detector sensitivity are not significantly wavelength dependent. This is a two wavelength scheme in which one wavelength carries the sensor information while the other carries the reference signal. As both wavelengths traverse the same path, the ratio of the two detected signals provides a link-insensitive output [6].

The third referencing technique discussed is a balanced bridge as illustrated in Figure 1-1 [6]. Two similar sources operating at the same wavelength are used; one modulated at a lower frequency (~1 kHz) and the other at a higher frequency (~10 kHz). The output of each source is connected to an optical fiber and directed to the bridge network which includes the intensity-modulating sensor. Two fibers carry the bridge output to separate detectors. After filtering, four output signals are detected. These signals are used to determine the sensor intensity modulation which is expressed by [6]

$$Sensor\ Modulation = \frac{A(1\ kHz)}{A(10\ kHz)} \cdot \frac{B(10\ kHz)}{B(1\ kHz)}. \tag{1.1}$$

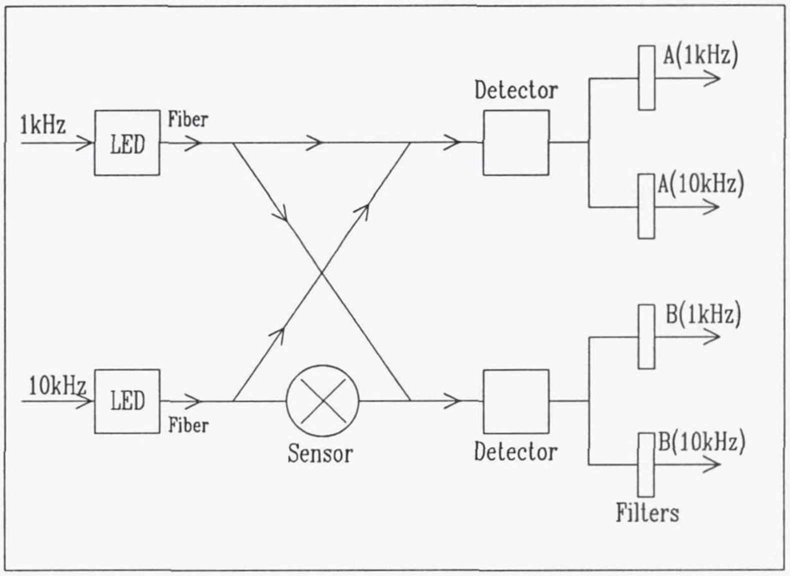

Figure 1-1: Single-wavelength referencing scheme using balanced bridge configuration.

1.1.1 Fiber Optic Sensor Concepts - Intensity Modulation

There are several types of intensity-modulated sensing concepts incorporating optical fibers. Multimode fibers or fiber bundles are more commonly used for this type of sensor. Three fiber optic sensor concepts utilize transmission, loss, and reflection [1]. All of these concepts will be discussed below in more detail.

Transmission Concept

The transmissive sensor varies the transmitted light intensity in a predictable manner relative to the sensed parameter. Pressure, force, displacement, and acceleration can be detected using this concept.

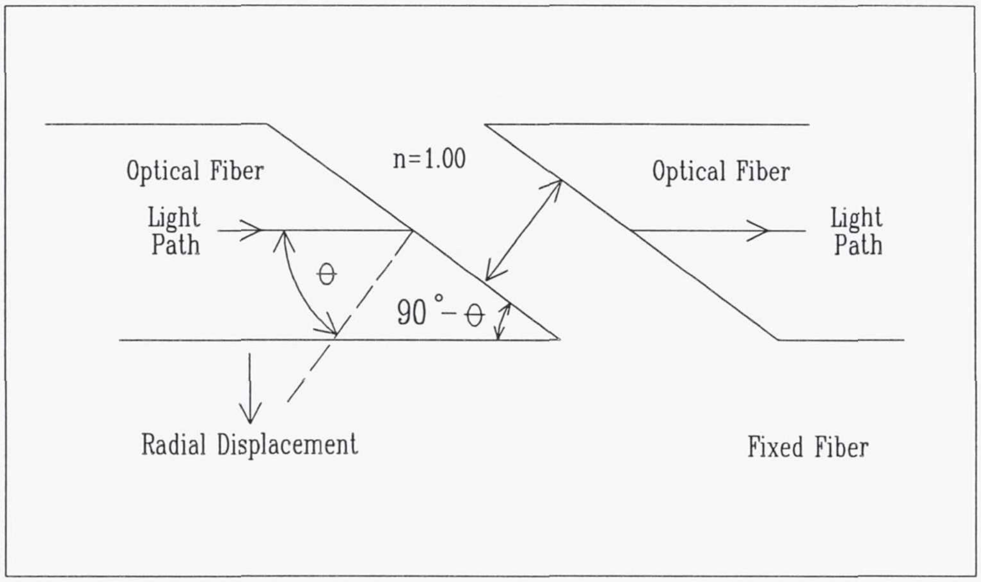

Figure 1-2: Fiber optic hydrophone.

One transmissive sensor detects radial displacement and is shown in Figure 1-2. Two multi-mode fibers are polished at an angle with respect to the fiber axis. Both fibers are in a frustrated total internal reflection (FTIR) configuration. Hence, light is coupled between the two fibers only when they are in close proximity with each other. The transmitted intensity is dependent on the distance between the fibers, thus producing an intensity modulated output. For a hydrophone, the gap width is made a function of the acoustical displacement using a diaphragm [7], [8]. Another displacement sensor uses two fibers which are polished normal to the fiber axis ($\theta = 0$), and again, one fiber moves radially while the other remains fixed. Absorptive gratings can be fabricated on the ends of the two fibers to increase sensitivity [9].

Loss - Microbend Concept

The microbend concept is rather simple. When an optical fiber is bent, it causes the output intensity to decrease due to the loss at the bend. Therefore, when an external force is applied to the apparatus shown in Figure 1-3, the output intensity will decrease. This output intensity is inversely related to the applied force. Because light is entirely confined to the fiber, the possibility of environmental contamination is eliminated. Temperature, acceleration, strain, displacement, vibration, and pressure are natural parameters to be measured using this technique [10], [11].

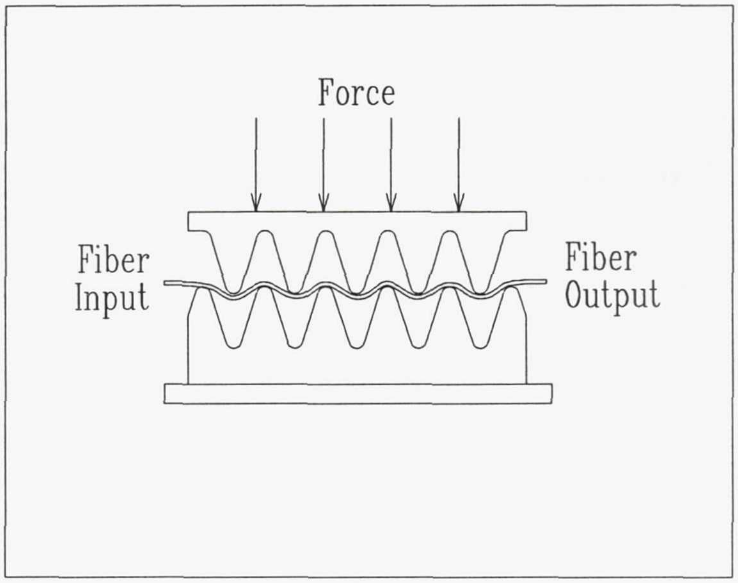

Figure 1-3: Microbend sensor concept.

Reflection Concept

The reflective sensor concept is conducive to measuring displacement in the axis of the fiber. Light propagating through an optical fiber is directed out the opposite end where it is reflected off a surface whose distance from the fiber end varies as a function of the sensed parameter. A portion of this reflected light, which is inversely proportional to the distance, re-enters the fiber and is directed to a detector [12], [13]. Film thickness and index of refraction may also be determined using this concept [14]. By replacing the mirror with a diaphragm pressure can be measured using this configuration.

1.1.2 Integrated Optic Sensor Concepts - Intensity Modulation

Several intensity-modulated integrated optic concepts have been developed utilizing micromachining techniques. The sensor concept discussed here involves a micromachined cantilever beam.

Cantilever Beam Concept

A cantilever beam [15] which has a waveguide fabricated on it, as shown in Figure 1-4, deflects when a force is applied. The beam deflection can be determined optically by the decrease in light coupled across the gap into the output guide. Thus, mechanical vibrations are directly converted into an intensity-modulated output [16]. Typical integrated optic devices are fabricated on silicon substrates having thick oxide isolation layers. Silicon oxynitride (SiON) films are deposited on the oxide and using photolithography are selectively etched to produce the desired device structure. For devices having large amplitude vibrations, the intensity modulation method described here is preferred. For lower amplitude vibrations, interferometric techniques are preferred [6].

For acceleration measurements, device sensitivity can be controlled by proper choice of the beam thickness, length, and foot mass. Thus, to detect small accelerations with greater accuracy, the beam tip thickness is decreased, or a foot mass is added to the beam tip to increase its deflection [15]. Cantilever beams can also be used to detect pressure, force, displacement [17], and acoustic signals [18].

1.2 Phase Modulation - Sensor Concepts

Phase modulation or interferometric techniques generally require single-mode components and coherent light sources. Using these techniques, phase shifts on the order of 10^{-4} radians can easily be detected, with shifts on the order 10^{-8} radians approaching detection limits [4]. These interferometric techniques convert the phase-modulated signal into an intensity-modulated signal.

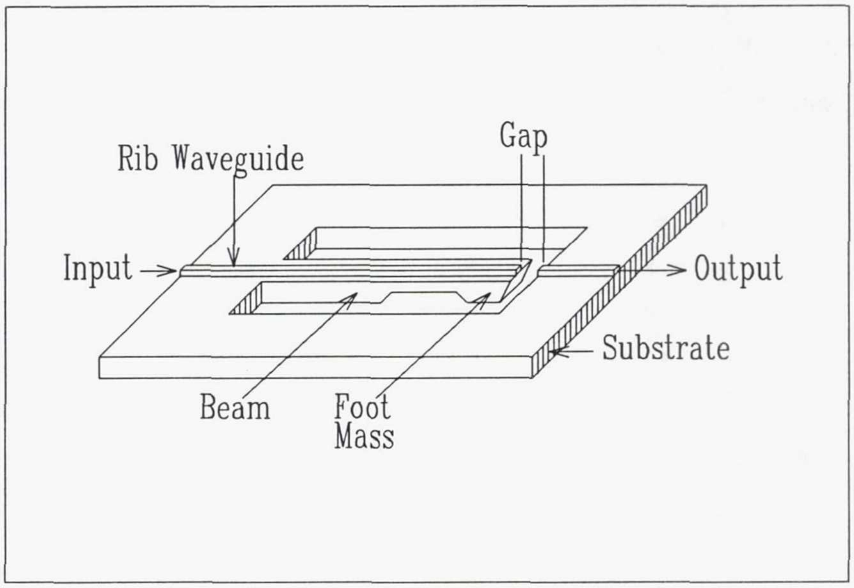

Figure 1-4: Cantilever beam - accelerometer configuration (foot mass).

Compared to intensity-modulated sensors, phase-modulated sensors are more complex. Also, there are some problems associated with this scheme. First, a change in the wavelength of the source can cause an undesired phase change. Another problem is that the output signal may be ambiguous [4] due to the interferometer's sinusoidal output. Phase shifts of 0, 2π, 4π, etc. are indistinguishable from each other unless properly referenced. Also, stability of the reference arm is critical, but difficult to maintain because environmental conditions may produce phase changes independent of the measurand. Finally, these sensors can only be effectively operated when the optical path difference between the sensor and reference arms is smaller than the coherence length of the source [19].

1.2.1 Fiber Optic Sensor Concepts - Phase Modulation

Fiber optic interferometers are very sensitive. A typical two-beam interferometer consists of a coherent light source coupled into two single-mode fibers. One fiber is the sensor arm which is affected by changes in the measured parameter. The other arm, the reference, is unaffected. When light from the two arms is recombined, their phase difference is converted into an intensity which depends in a sinusoidal manner upon the phase shift. Four interferometric techniques to be discussed are: (1) Mach-Zehnder, (2) Michelson, (3) Fabry-Perot, and (4) Sagnac [1].

Mach-Zehnder Interferometer

A Mach-Zehnder interferometer is a two-beam interferometer which splits the input light into reference and sensor arms as shown in Figure 1-5. Light from the two arms is then recombined and the output detected. A phase shift between the two paths results from measurand induced changes in the refractive index and/or length of the sensing arm. The output intensity can be expressed as

$$I = \frac{I_o}{2}\left(1 + \cos\phi\right), \tag{1.2}$$

where I_o is the input intensity and ϕ is the phase shift. Sensitivity to small changes in ϕ is maximized at $\phi = \frac{\pi}{2}$, and is zero at $\phi = 0, \pi$. Assuming the index of the sensor and reference arm is the same ($n_s = n_r = n$), the phase shift is given by

$$\phi = \frac{2\pi}{\lambda_o} nL, \tag{1.3}$$

where λ_o is the free-space wavelength and L is the length difference between the two arm lengths ($L_s - L_r$). A change in the measurand induces a phase shift change of

$$\Delta\phi = \frac{2\pi}{\lambda_o}\left(\Delta n L + n \Delta L\right). \tag{1.4}$$

This approach is widely used for acoustic sensing [1],[10].

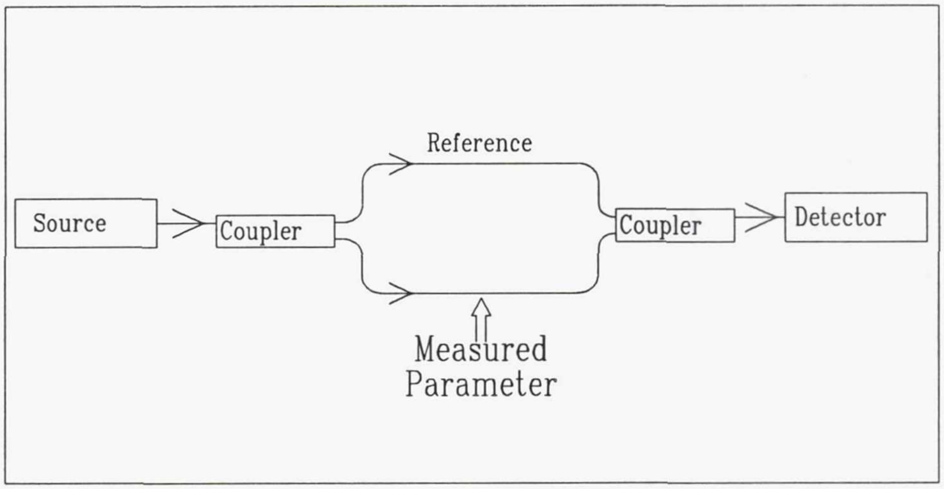

Figure 1-5: Fiber optic Mach-Zehnder interferometer.

Michelson Interferometer

The Michelson interferometer is similar to the Mach-Zehnder configuration, except reflected light is used for detection as illustrated in Figure 1-6. The sensor and reference fibers have mirrored ends which reflect the light back to the detector. This gives twice the sensitivity of the Mach-Zehnder interferometer, i.e.

$$\phi = \frac{4\pi}{\lambda_o} nL. \tag{1.5}$$

Care must be taken when using this type of interferometer in a fiber optic sensor configuration because the reflected light is fed back into the light source. For lasers, this feedback can cause instability, but isolators can be used to prevent this problem. A temperature sensor based on an all-fiber Michelson interferometer has been reported [20].

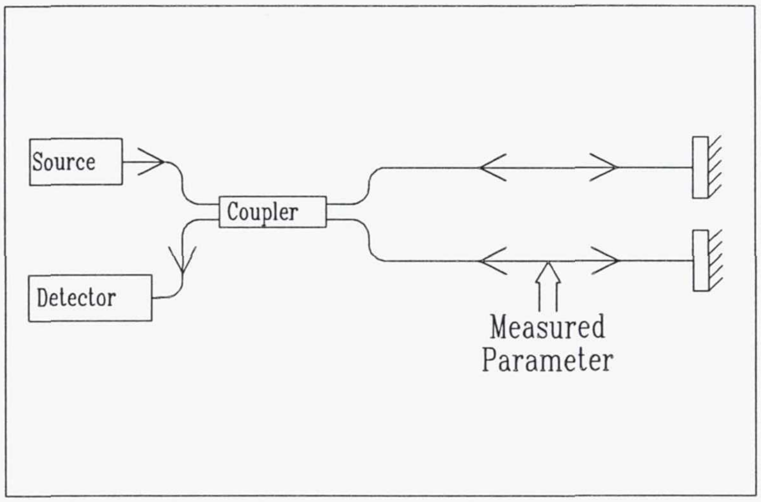

Figure 1-6: Fiber optic Michelson interferometer.

Fabry-Perot Interferometer

Unlike the two-beam interferometers previously discussed, a Fabry-Perot interferometer has a single path. Incident light encounters two partially reflecting parallel mirrors separated by a gap as illustrated in Figure 1-7. Interference occurs as the incident beam is successively reflected between the mirrors. Changes in the gap width l alter these reflections. Interference is determined by the one-way phase shift across the gap, which is defined by [21]

$$\phi = \frac{2\pi n l \cos\theta'}{\lambda_o}, \tag{1.6}$$

where n is the index of the material between the mirrors, and θ' is the angle of incidence inside the cavity. An important characteristic of a Fabry-Perot interferometer is its finesse. Defined as the ratio of the separation of adjacent fringes and the half-intensity width, finesse can be written as [21]

$$\mathcal{F} = \frac{\pi\sqrt{R}}{1-R}, \tag{1.7}$$

where R is the reflectivity of the mirrors, hence, the higher the reflectivity, the higher the finesse. Either the reflected or transmitted light from a Fabry-Perot interferometer may be used in a sensing application. The ratios of the reflected and transmitted intensities to the incident intensity are given by [21]

$$\frac{I_t}{I_i} = \frac{1}{1 + F \sin^2 \phi}, \tag{1.8}$$

and

$$\frac{I_r}{I_i} = \frac{F \sin^2 \phi}{1 + F \sin^2 \phi} \tag{1.9}$$

where

$$F = \frac{4R}{1 - R^2}. \tag{1.10}$$

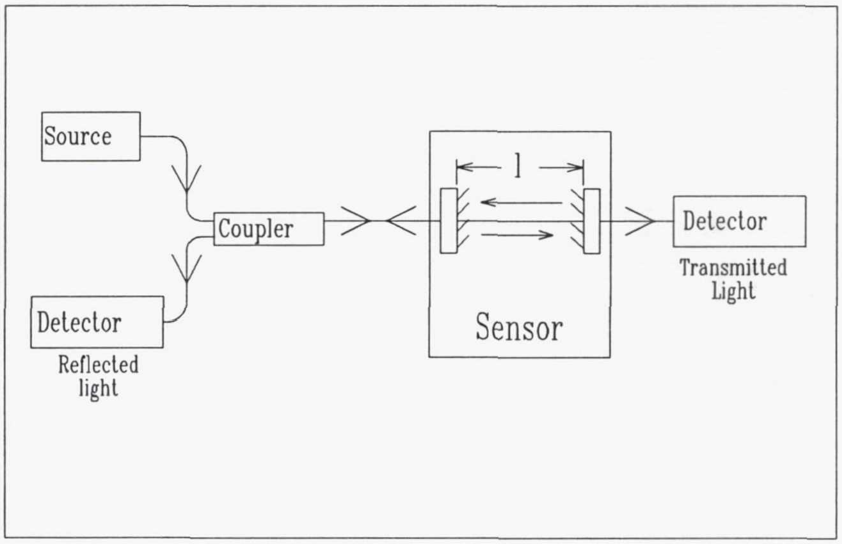

Figure 1-7: Fiber optic Fabry-Perot interferometer.

Sagnac Interferometer

Sagnac interferometers are most often used for rotation sensing. The source light is split into two beams which propagate in opposite directions around the closed path of a coil as shown in Figure 1-8. While held stationary, no phase shift is detected. However, when the fiber ring is rotated, there is a phase shift which is expressed by [22]

$$\phi = \frac{4\pi LR}{\lambda_o c}\omega, \tag{1.11}$$

where L is the fiber length, R the coil radius, ω the rotation rate, λ_o the free-space wavelength, and c the speed of light. Fiber gyroscopes are based on this concept [23] and are also amenable to integrated optics [24]. Electric and magnetic fields [25], [26] can be detected using a Sagnac interferometer as well as leaks in long-distance gas or fluid-filled lines [27], [28].

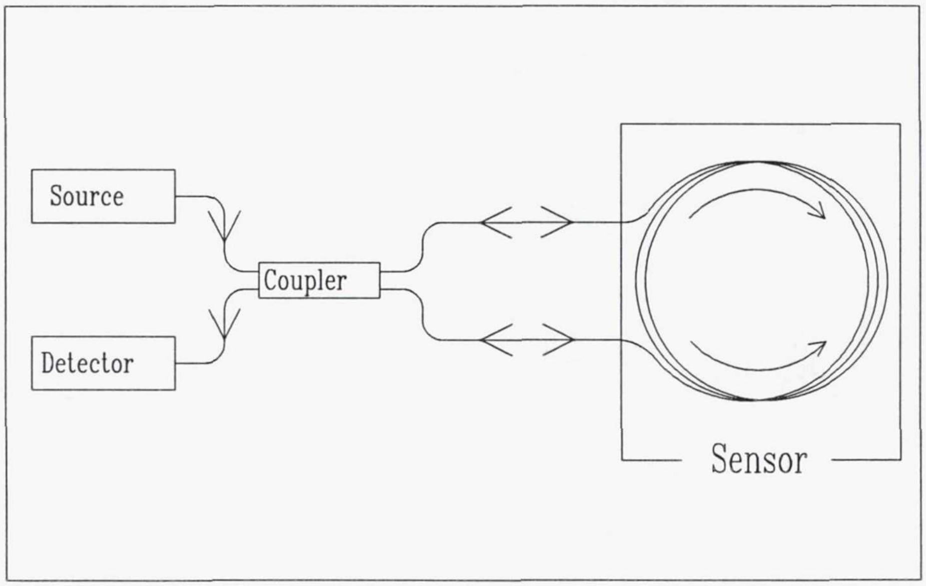

Figure 1-8: Fiber optic Sagnac interferometer.

1.2.2 Integrated Optic Concepts - Phase Modulation

Reliability is expected to be improved and cross-sensitivity reduced using integrated optic phase-transduced interferometric sensors [29]. The optical paths in an integrated optic phase-modulated sensor are fabricated in close proximity on a single substrate.

Hence, these devices are expected to be more stable than fiber interferometers with respect to environmental changes. Silicon [30], [31], gallium arsenide, and lithium niobate are commonly used integrated optic substrates since all have well-established fabrication techniques and possess excellent waveguiding properties. Because phase shift is to be detected, single-mode components are most often used. Two phase measuring interferometric techniques will be discussed with respect to integrated optic structures: Mach-Zehnder and Michelson.

Mach-Zehnder Interferometer

This type of interferometer can be used in a variety of sensor configurations. These include but are not limited to: pressure, strain, acoustic wave, temperature, high-voltage, and electric field sensing. Some of these will be discussed further.

Several papers have been published describing pressure sensors utilizing the Mach-Zehnder interferometer [32],[33],[34],[35],[36]. Generally, the sensing arm is fabricated on a micromachined diaphragm. Pressure applied to the diaphragm causes it to deform, thus inducing a strain in the waveguide which causes an index of refraction change due to the photoelastic effect.

Another parameter to be sensed is the distance from the edge of a guide to an external reflector [37]. Hydrogen can be detected using this scheme [38] when the optical refractive index of a Pd film on a Y-cut $LiNbO_3$ substrate changes due to hydrogen absorption and desorption. As a last example, a temperature sensor has been discussed in the literature where the path length change between the two arms is used to deduce temperature [39].

Michelson Interferometer

Using a Michelson interferometer, cantilever beam deflections [40], [41] can be measured. Displacement of an external reflector can also be measured [42],[43], similar to a Mach-Zehnder. An integrated optic displacement sensor [43] is illustrated in Figure 1-9. Two mirrors are used: one attached to the object being displaced, the other onto the chip edge. Light enters the input path where it is divided between the reference arm and the sensing arm by a coupler. The sensor path reflects off the object mirror and combines with the reflected reference light where it is directed toward the output waveguide as an intensity-modulated signal. Varying this configuration, temperature, humidity [44], and pressure [45] can be detected as well.

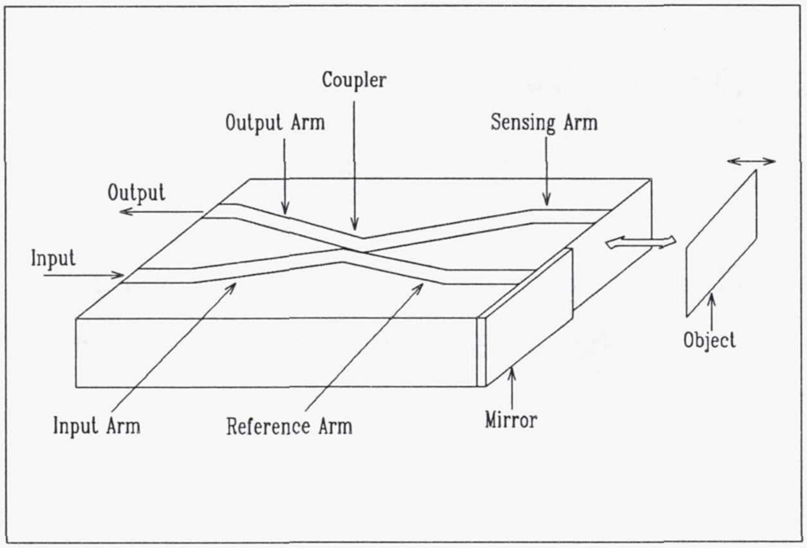

Figure 1-9: Displacement sensor using a Michelson interferometer.

1.3 Wavelength Modulation

Sensor configurations using wavelength modulation generally utilize a broadband source, wavelength modulator (transducer), and spectrometer, along with detection electronics [6]. Thus, demodulation is generally more complex for this scheme [4]. Multimode fibers are often used to transmit the sensor signal. Using wavelength encoding, sensor output is inherently less susceptible to loss variations in the fibers and connectors.

A typical wavelength-modulated sensor scheme is illustrated in Figure 1-10. A broadband light source, with spectrum $W_o(\nu)$, where ν is the wavenumber, is coupled to a

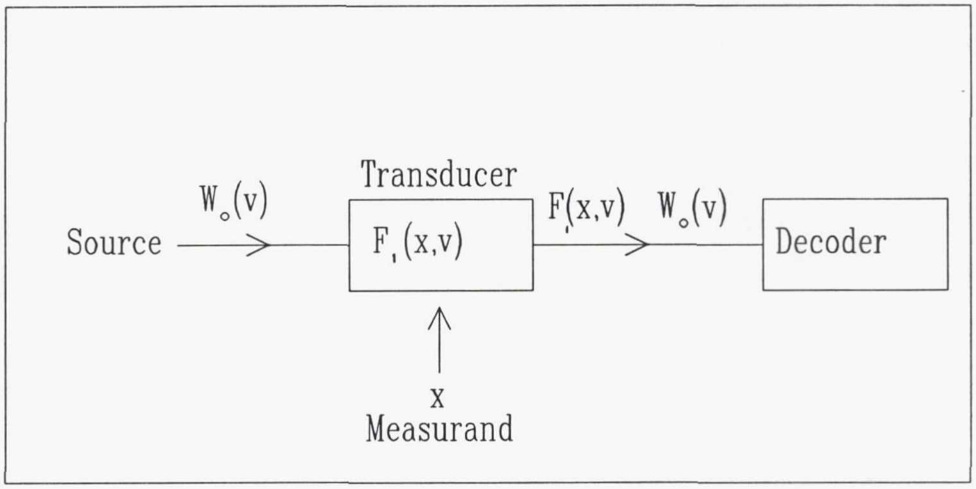

Figure 1-10: Typical wavelength-modulated sensor scheme.

fiber and directed toward the transducer. The value x of the parameter being sensed determines the spectral transmission $\mathrm{F}_1(x,\nu)$, thus filtering the input spectrum. This filtered spectrum, $\mathrm{F}_1(x,\nu)\mathrm{W}_o(\nu)$, contains the encoded measurement information and is directed to the decoder where the value of x is determined [46].

1.3.1 Fiber Optic Sensor Concepts - Wavelength Modulated

Fabry-Perot

A Fabry-Perot temperature sensor can be fabricated directly on the end of an optical fiber [47], [48] as shown in Figure 1-11. The silicon Fabry-Perot etalon is sputter deposited on the fiber tip along with some protective overlayers. As the temperature increases, the etalon thickness and index of refraction increase, thereby shifting the reflected spectrum to longer wavelengths. The resonant wavelengths of the etalon are expressed as [47]

$$\lambda_m = \frac{2nl}{m}, \tag{1.12}$$

where n is the index of refraction of the silicon, l is its thickness, and m is an integer. Quantitatively, the change in resonant wavelength as a function of temperature is given by [47]

$$\Delta\lambda_m = \lambda_m \left(\frac{1}{n}\frac{dn}{dT} + \frac{1}{l}\frac{dl}{dT}\right)\Delta T. \tag{1.13}$$

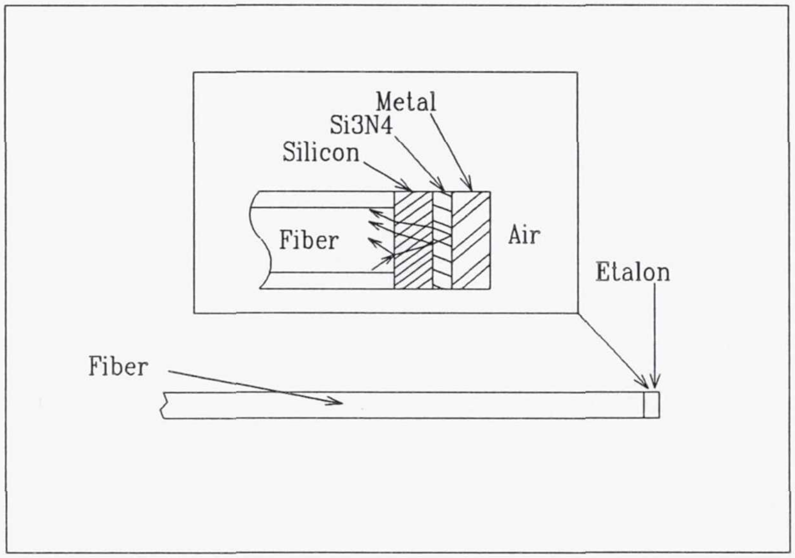

Figure 1-11: Fiber optic Fabry-Perot temperature sensor.

Using the configuration illustrated in Figure 1-12, pressure can be measured. Light is incident on the Fabry-Perot cavity which deforms when pressure is applied to the diaphragm. The reflected light is wavelength modulated by changes in this cavity's width [49]. If the device is properly shielded, external electric fields can be detected by the electrostatic force exerted on the diaphragm [50].

Encoder

A 10-bit digital optical position encoder has been fabricated [51] and is shown in Figure 1-13. Light from a broadband source is dispersed across the channels of a reflective code plate by the graded-index (GRIN) rod lens and prism grating structure. Wavelengths

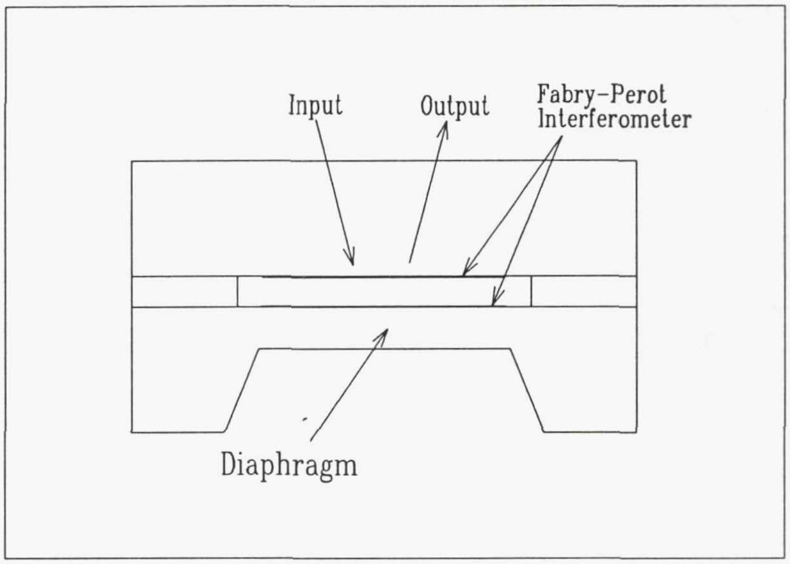

Figure 1-12: Pressure sensor based on wavelength modulation.

incident on a channel in the logic-zero state are absorbed. Alternatively, wavelengths incident on a channel in the logic-one state are reflected off the code plate and retransmitted to the input/output fiber. This reflected light is then directed by a coupler to a separate encoder output fiber which transmits it to a spectrum analyzer.

1.3.2 Integrated Optic Sensor Concepts - Wavelength Modulation

Ring Resonator

A micromachined ring resonator pressure sensor is shown in Figure 1-14. Light propagates from the input channel waveguide through the first Y-branch and is split at the second Y-branch. A portion of this light then travels around the ring where it crosses the diaphragm. The light continues around the ring to the first Y-branch and interferes with the incoming light. The effective index of the ring, n_e, is altered when the diaphragm is

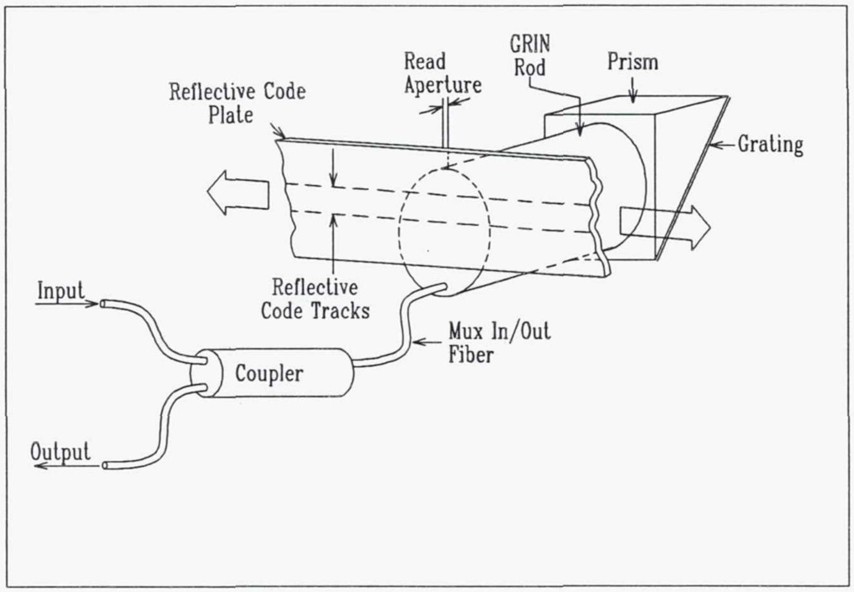

Figure 1-13: Optical position encoder.

perturbed by an applied pressure. The round trip phase shift of the ring is given by [52]

$$\phi = \frac{2\pi}{\lambda_o} \int_0^L n_e(l)dl, \tag{1.14}$$

where λ_o is the wavelength of the source and n_e is integrated around the perimeter of the ring having length L. At resonance, the ring and input light constructively interfere such that $\phi = 2\pi m$, where m is an integer, which causes the transmissivity of the ring resonator to be a maximum. When $\phi = 2\pi(m+\frac{1}{2})$, the transmissivity is a minimum. The sensor's response to pressure is linear with a sensitivity of 0.0094 rad/kPa for the TM mode [52]. This sensor exhibits cross-sensitivity to temperature which may be reduced by shortening the path length [53]. The ring resonator configuration can be used to measure other parameters by replacing the diaphragm in Figure 1-14 with an appropriate sensing mechanism.

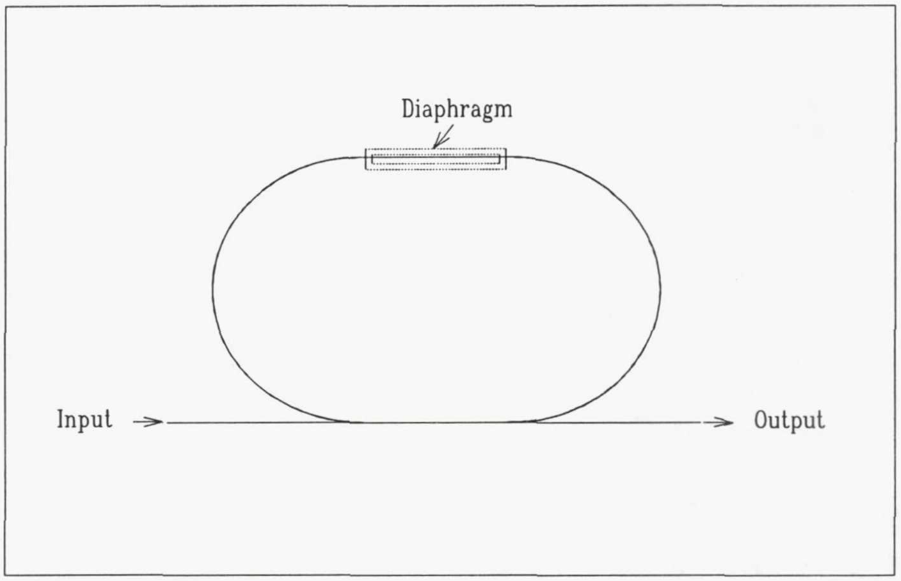

Figure 1-14: Integrated optic ring resonator interferometer.

1.4 Polarization Modulation - Sensor Concepts

Polarization modulation is another concept used to encode and recover the measurand [19]. Analogous to the previous methods, the relevant physical parameter to be measured is converted into a polarization change, which may be due to electro-optic or elasto-optic effects. Polarization modulation techniques have been advancing due to commercially available polarization-maintaining fibers. These highly birefringent fibers can maintain the state of linearly polarized light [4].

1.4.1 Fiber Optic Sensor Concepts - Polarization Modulation

Polarization-maintaining fibers can be used as temperature sensors due to the birefringence changes with temperature. For current and magnetic field sensing [54], [55], low-birefringence fibers are used to exploit the Faraday effect. This effect is a polarization rotation which occurs when a magnetic flux is in the same direction as the light propagating in an optical fiber [4]. The rotation, θ, is expressed as

$$\theta = V \int_{o}^{L} \overline{B} \cdot d\bar{l}, \tag{1.15}$$

where V is the material Verdet constant, $\overline{B}$ is the magnetic flux density, and L the optical path length. A compact current sensor using this effect has been fabricated using yttrium iron garnet with 0.7°/A sensitivity [56].

1.4.2 Integrated Optic Concepts - Polarization Modulation

Using the integrated optic nanomechanical effect, polarization can be modulated as a function of the measured parameter [57]. An example of this configuration is shown in Figure 1-15. This effect causes a change in the TE and TM effective indices of the guide. When a small nonabsorbing dielectric plate is positioned above the guide, separated by a gap ($d < \lambda$), it will interact with the evanescent field of the guide. This interaction causes the effective index of the guide to vary dependent upon the distance d. Because the change in effective index for the TE and TM modes differs, a phase shift between the two modes is induced. Using a polarizer oriented at 45°, the phase shift is converted to an intensity modulated signal. Acoustical sensing can be performed using this method [57].

Polarization sensors can also be used for magneto-optical disk pickup where detection of the disk state is performed using a Faraday rotator. Such a sensor has been fabricated with all its components integrated on one chip [58].

1.5 Time/Frequency Modulation Sensor Concepts

Time and frequency modulation are so closely related that they are being addressed together. An advantage to these modulation schemes is high immunity to cable and connector effects. As opposed to intensity-modulated schemes, source intensity fluctuations

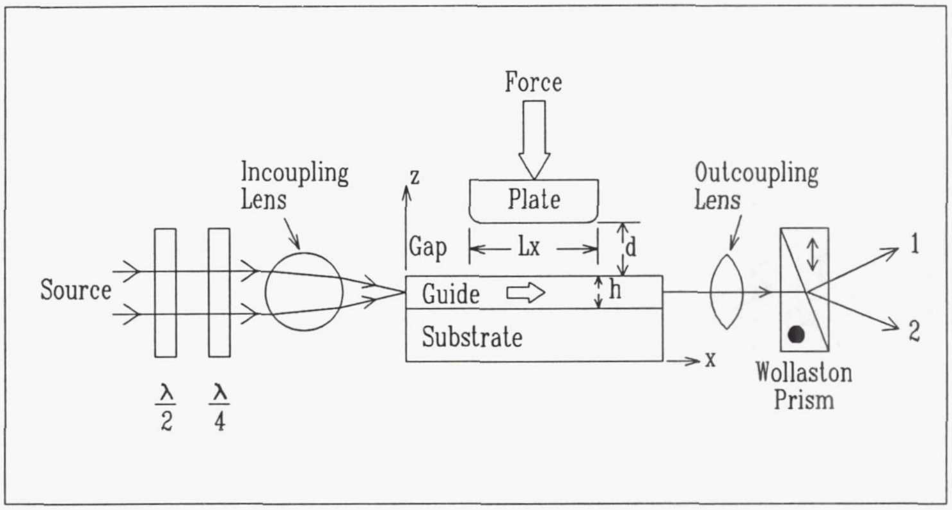

Figure 1-15: Polarimeteric interferometer where effective-index is affected by force applied to plate.

are not as critical when using a frequency-modulated sensor [59]. A frequency-modulated sensor can be constructed from a vibrating element such that its resonant frequency can be made to vary with respect to the measurand.

1.5.1 Fiber Optic Sensor Concepts - Time Modulation

Fluorescent Time Rate of Decay Concept

This technique uses pulses of broadband light to excite a fluorescent material located at the end of a fiber as illustrated in Figure 1-16. When the excitation ceases, the energy emitted from the material decays exponentially with time constant τ. As decay time is related to temperature, a temperature sensor can be fabricated using this technique [60], [61]. Over the range -70°C to 350°C the sensitivity is typically better than -0.3%/°C [60]. An interesting property of the decay signal is that its spectrum is wavelength-shifted with respect to the source. This wavelength shift is temperature sensitive, and hence can be used to deduce temperature. Oxygen can also be detected using this fluorescence time rate of decay principle [62].

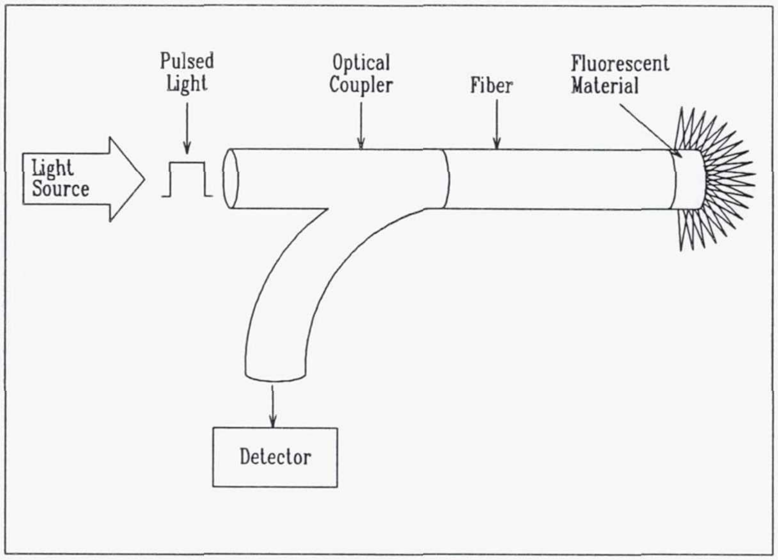

Figure 1-16: Fluorescent time rate of decay temperature sensor.

Optical Time Domain Reflectometry

Similar to the technique above, a short pulse is launched into a fiber and the returned signal detected. The time resolution of the backscattered light is linearly dependent on the measurand. For communications applications, time resolution of the backscattered power determines the spatial distribution of the fiber attenuation. This provides information regarding fiber breaks, poor splices, and unusually lossy fiber sections [63].

1.5.2 Fiber Optics - Frequency Modulation

Resonant Microstructure

A fiber optic pressure sensor has been fabricated which exploits the pressure dependent resonance frequency of a silicon diaphragm [64]. The microstructure is excited into resonance, through the thermooptic effect, by the modulated light from a fiber as shown in Figure 1-17. The vibration amplitude is measured by a displacement sensor, shown in Figure 1-18. Light from one fiber travels across a gap of width l to the opposite fiber.

A shutter attached to the vibrating microstructure is oriented perpendicular to the fiber axis and modulates the light transmitted from the input to the output fiber. The distance between the central axis of the fiber and the bottom of the shutter is denoted by h. The vibration amplitude of the microstructure, h_o where $h(t) = h_o \sin(2\pi f t)$, is determined from the amplitude of the transmitted light modulated at the vibration frequency, f. The frequency of the excitation is adjusted to maximize h_o, thereby determining the resonant frequency and hence the applied pressure.

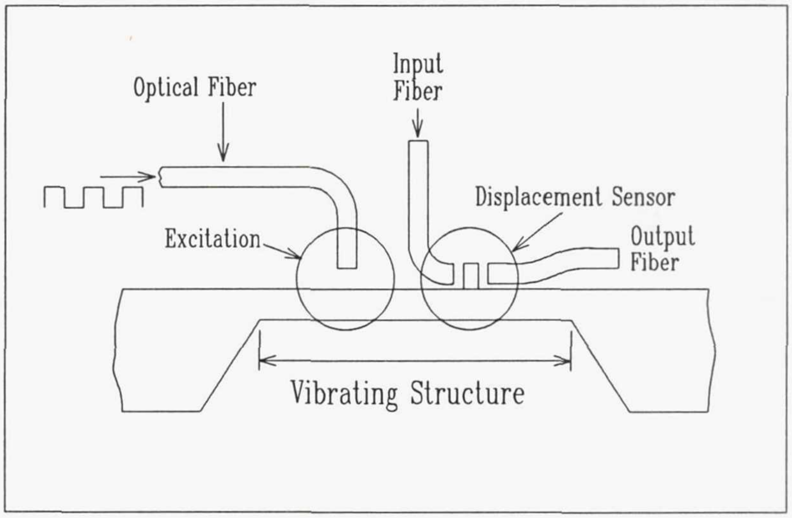

Figure 1-17: Frequency-modulated optical pressure sensor.

Laser Doppler Velocimetry

To measure gas or fluid flows, Laser Doppler Velocimetry (LDV) is often used. When laser light is scattered by moving particles in a flow stream, it experiences a Doppler frequency shift. The Doppler shifted frequency is [65]

$$f = \frac{2v}{\lambda_o} \cos\theta, \tag{1.16}$$

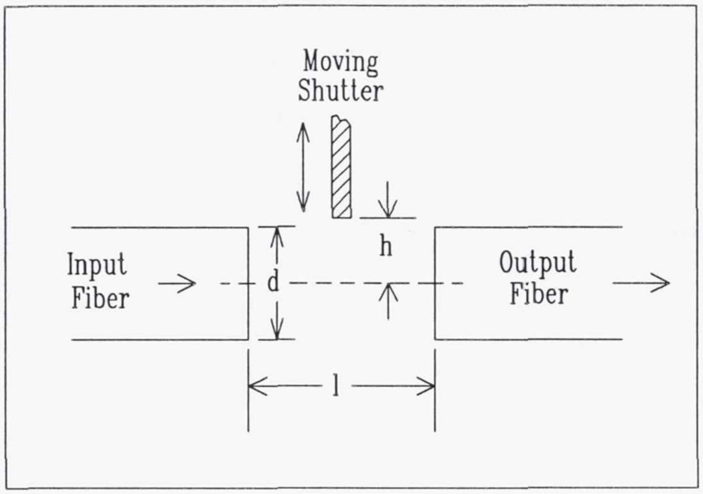

Figure 1-18: Displacement sensor used with pressure sensor.

where λ_o is the laser wavelength, v is the flow velocity, and θ is the angle between the incident laser beam and the flow. This scheme is conducive to both fiber optics [4] and integrated optics [66] and can be used to measure flows in wind tunnels and pipelines [10].

1.5.3 Integrated Optics - Frequency Modulation

Bridge resonators

Strain, pressure, vibration, and displacement are common parameters determined using this modulation scheme [10]. For resonant frequency sensors, a high quality factor, Q, is desired. Losses from friction in the medium surrounding the resonator reduce Q, therefore, operating in vacuum will increase Q [67]. Since resonators are strongly affected by temperature change, compensation methods are often needed to prevent thermal cross-sensitivity [68].

Large amplitude vibrations of the cantilever beam were previously discussed in the integrated optic intensity-modulated sensor section. Here, a microbridge with low amplitude vibrations will be discussed. A microbridge, illustrated in Figure 1-19, is excited by intensity-modulated light incident on the structure. This incident light produces a thermal stress causing the structure to vibrate. When the incident light frequency matches the bridge's natural resonance frequency, the maximum output amplitude is achieved [69]. The bridge's fundamental undamped resonance frequency is expressed by [69]

$$f_b = 1.028\frac{t}{L_b^2}\sqrt{\frac{kE_s}{\rho_s}\left(1 + 0.295L_b^2\frac{\varepsilon}{t^2}\right)} \tag{1.17}$$

where t is the thickness of the beam, L_b is the bridge length, k is a coefficient related to the beam components, ρ_s is the beam density, E_s is the Young's modulus of the substrate, and ε is the longitudinal tensile strain of the bridge. This vibration amplitude is detected optically using an integrated optic interferometer [70], [68]. Measurand-induced changes in the strain of the device are detected as changes in the device resonant frequency.

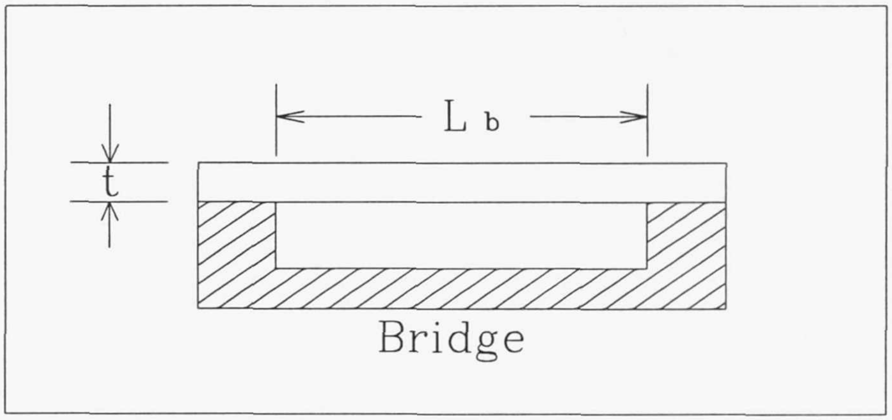

Figure 1-19: Bridge resonator.

Microresonators can be used to determine chemical components, small masses, temperature, pressure [71], [72], and vibration. For a prototype pressure sensor [72] operating in the 0 - 300 kPa range with an 18 kHz span, the pressure sensitivity was $\sim$ 0.006 kHz/kPa. A vibration sensor can be used to detect Young's modulus and built-in stress of thin deposited films [73]. Using GaAlAs, a cantilever beam along with a light source and detector has been integrated on one chip [74].

Self-oscillation techniques may also be used [69]. Self-oscillation refers to a device which oscillates when illuminated with a CW light source and thus is more practical because only one unmodulated laser source is required for both the excitation and interrogation of the microresonator. This oscillation frequency is determined by the mechanical properties of the structure and varies with respect to the measurand [71], [69], [75].

1.6 Summary

Five modulation techniques have been discussed: intensity, phase, wavelength, polarization, and time/frequency.

Intensity-modulated sensors are the simplest to implement. However, they must be properly referenced to avoid source, connector, and detector fluctuations from corrupting the sensor output. Interferometric techniques are very sensitive and convert phase change into an intensity-modulated signal. Wavelength-modulated sensors use reflected or transmitted wavelength shift to deduce the measurand and are therefore less affected by loss variations. However, errors can be produced from source wavelength shift caused by changes in temperature. Polarization can be modulated with respect to the measurand, such as current or magnetic field strength, by exploiting the Faraday effect. Time and frequency-modulated sensors are inherently immune to fiber and connector losses. However, fluorescent time rate of decay sensors have high insertion loss [76] and microresonators are strongly temperature dependent.

It is hoped that this chapter has provided the reader with an overview of sensor concepts that have been developed to date, with the references given to provide further details.

Bibliography

[1] D.A. Krohn, Fiber Optic Sensors Fundamentals and Applications, Instrument Society of America, North Carolina, 1988.

[2] C.M. Davis et. al., Fiber Optic Sensor Technology Handbook, Dynamic Systems, Reston, Virginia, 1982.

[3] B. Culshaw, "Optical Systems and Sensors for Measurement and Control," J. Phys. E: Sci. Instrum., Vol. 16, pp. 978-986, 1983.

[4] S. Medlock, "Review of Modulating Techniques for Fibre Optic Sensors," J. Opt. Sensors, Vol. 1, No. 1, pp. 43-68, 1986.

[5] J.P. Dakin, "Multiplexed and Distributed Optical Fibre Sensor Systems," J. Phys. E: Sci. Instrum., Vol. 20, pp. 954-965, 1987.

[6] B. Culshaw and J. Dakin, ed., Optical Fiber Sensors: Systems and Applications, Vol. II, Artech House, Inc., MA, 1989.

[7] W.B. Spillman Jr., D.H. McMahon, "Frustrated–Total-Internal-Reflection Multimode Fiber Optic Hydrophone," Appl. Opt., Vol. 19, pp. 113-117, 1980.

[8] T.G. Giallorenzi et. al. "Optical Fiber Sensor Technology," IEEE. J. Quant. Electron., Vol. QE-18, No. 4, 1982.

[9] D.H. McMahon, A.R. Nelson, and W.B. Spillman Jr., "Fiber Optic Transducers," IEEE Spectrum, pp. 24-29, 1981.

[10] G.D. Pitt, "Optical-Fibre Sensors," IEE Proceedings, Vol. 132, Pt. J., No. 4, pp. 214-248, 1985.

[11] J.W. Berthold III, "Historical Review of Microbend Fiber Optic Sensors," Proc. 10th Optical Fibre Sensors Conference, pp. 182-185, 1994.

[12] C.D. Kissenger, and B. Howland, "Fiber Optic Displacement Measuring Apparatus," U.S. Patent 3,940,608, Feb. 24, 1976.

[13] A.K. Bejczy, H.C. Primus, and W.A. Herman, "Fiber Optic Proximity Sensor," NASA Tech Briefs, Vol. 4, No.3, Item 63, JPL Report NPO-14653/ 30-4279, March 1980.

[14] W.V. Sorin, "High Resolution Optical Fiber Reflectometry Techniques," Distributed and Multiplexed Fiber Optic Sensors II, Proc. SPIE, Vol. 1797, pp. 109-118, 1992.

[15] K.E. Burcham, G.N. De Brabander, and J.T. Boyd, "Micromachined Silicon Cantilever Beam Accelerometer Incorporating an Integrated Optical Waveguide," Integrated Optics and Microstructures, Proc. SPIE, Vol. 1793, pp. 12-18, 1992.

[16] H. Bezzaoui and E. Voges, "Integrated Optics Combined with Micromechanics on Silicon," Sensors and Actuators A, Vol. 29, pp. 219-223, 1991.

[17] D. Uttamchandani, D. Liang, and B. Culshaw, "A Micromachined Silicon Accelerometer with Fibre Optic Interrogation," Integrated Optics and Microstructures, Proc. SPIE, Vol. 1793, pp. 27-33, 1992.

[18] S. Wu and H.J. Frankena, "Integrated Optical Sensors using Micromechanical Bridges and Cantilevers," Integrated Optics and Microstructures, Proc. SPIE, Vol. 1793, pp. 83-89, 1992.

[19] Y.N. Ning, K.T.V. Grattan, W.M. Wang and A.W. Palmer, "A Systematic Classification and Identification of Optical Fibre Sensors," Sensors and Actuators A, Vol. 29, pp. 21-36, 1991.

[20] M. Corke, A.D. Kersey, D.A. Jackson, and J.D.C. Jones, "All fibre 'Michelson' Thermometer," Electron. Lett., Vol. 19, pp. 471-473, 1983.

[21] M. Born and E. Wolf, Principles of Optics, Pergamon, Oxford, 1970.

[22] C.M. Davis, E.F. Carome, M.H. Weik, S. Ezekiel, R.E. Einzig, Fiberoptic Sensor Technology Handbook, Optical Technologies, Inc., Herndon, Virginia, 1986.

[23] G. Trommer, E. Hartl, and R. Müller, "Progress in Passive Fiber Optic Gyroscope Development," Proc. 10th Optical Fibre Sensors Conference, pp. 438-444, 1994.

[24] R.T. Kersten, "Integrated Optical Sensors," Proceedings of the NATO Advanced Study Instit Kluwer Academic Publishers, Massachusetts, pp. 243-266, 1987.

[25] J. Blake, P. Tantaswadi and R.T. de Carvalho, "In-Line Sagnac Interferometer for Magnetic Field Sensing," Proc. 10th Optical Fibre Sensors Conference, pp. 419-422, 1994.

[26] R.T. de Carvalho and J. Blake, "Simultaneous Measurement of Electric and Magnetic Fields using a Sagnac Interferometer," Proc. 10th Optical Fibre Sensors Conference, pp. 411-414, 1994.

[27] J.P. Kurmer, S.A. Kingsley, J.S. Laudo, and S.J. Krak, "Applicability of a Novel Distributed Fiber Optic Acoustic Sensor for Leak Detection," Distributed and Multiplexed Fiber Optic Sensors II, Proc. SPIE, Vol. 1797, pp. 63-71, 1992.

[28] J. Breguet, J.P. Pellaux, and N. Gisin, "Photoacoustical Detection of Trace Gases with an Optical Microphone," Proc. 10th Optical Fibre Sensors Conference, pp. 457-460, 1994.

[29] A. Enokihara, M. Izutsu, and T. Sueta, "Integrated-Optic Fluid Sensor Using Heat Transfer," Appl. Opt., Vol. 27, No.1, pp. 109-113, 1988.

[30] J.C. Greenwood, "Silicon in Mechanical Sensors," J. Phys. E: Sci. Instrum, Vol. 21, pp. 1114-1128, 1988.

[31] K.E. Petersen, "Silicon as a Mechanical Material," Proc. IEEE, Vol. 70, pp. 420-455, 1982.

[32] M. Ohkawa, M. Izutsu, and T. Sueta, "Integrated Optic Pressure Sensor on Silicon Substrate," Appl. Opt., Vol. 28, No. 23, pp. 5153-5157, 1989.

[33] K. Fischer, J. Müller, R. Hoffmann, F. Wasse, and D. Salle, "Elastooptical Properties of SiON Layers in an Integrated Optical Interferometer Used as a Pressure Sensor," J. Lightwave Tech., Vol. 12, No. 1, pp. 163-169, 1994.

[34] A. Vadekar, A. Nathan, and W.P. Huang, "Analysis and Design of an Integrated Silicon ARROW Mach-Zehnder Micromechanical Interferometer," J. Lightwave Tech., Vol. 12, No. 1, pp. 157-162, 1994.

[35] C. Wagner, "Optical Pressure Sensor Based on a Mach-Zehnder Interferometer Integrated with a Lateral a-Si:H p-i-n Photodiode," IEEE Photon. Tech. Lett., Vol. 5, No. 10, pp. 1257-1259, 1993.

[36] A. Nathan, Y. Bhatnagar, A. Vadekar, and W. Huang, "Fabrication of a Silicon Mach-Zehnder Interferometer for Mechanical Measurands," Integrated Optics ad Microstructures, Proc. SPIE, Vol. 1793, pp. 19-26, 1992.

[37] D. Peters, K. Fischer and J. Müller, "Integrated Optics Based on Silicon Oxynitride Thin Films Deposited on Silicon Substrates for Sensor Applications," Sensors and Actuators A, 25-27, pp. 425-431, 1991.

[38] A. Bearzotti, C. Caliendo, E. Verona, and A. D'Amico, "Integrated Optic Sensor for the Detection of H_2 Concentrations," Sensors and Actuators B, Vol. 7, pp. 685-688, 1992.

[39] L.M. Johnson, F.J. Leonberger, and G.W. Pratt, "Integrated Optical Temperature Sensor," Appl. Phys. Lett., Vol. 41, No. 2, pp. 134-136, 1982.

[40] J. Wilson and J.F.B. Hawkes, Optoelectronics: An Introduction , 2nd edition, Prentice Hall Int. Ltd., UK, pp. 239-241, 1989.

[41] H. Wölfelschneider et. al., "Optically Excited and Interrogated Micromechanical Silicon Cantilever Structure," Fiber Optic Sensors II, Proc. SPIE, Vol. 798, pp. 61-66, 1987.

[42] S. Valette, S. Renard, J.P. Jadot, P. Gidon, and C. Erbeia, "Silicon-Based Integrated Optics Technology for Optical Sensor Applications," Sensors and Actuators, A21-A23, pp. 1087-1091, 1990.

[43] M. Izutsu, A. Enokihara, and T. Sueta, "Optical-Waveguide Micro-Displacement Sensor," Electron. Lett., Vol. 18, No. 20, pp. 867-868, 1982.

[44] M. Izutsu, A. Enokihara, and T. Sueta, "Integrated Optic Temperature and Humidity Sensors," J. Lightwave Tech., Vol. LT-4, No. 67, pp. 833-836, 1986.

[45] M. Izutsu, A. Enokihara, N. Mekada, and T. Sueta, "Optical-Waveguide Pressure Sensor," European Conference on Integrated Optics, Firenze, pp. 144-146, 1983.

[46] R. Ulrich, "Theory of Spectral Encoding for Fiber-Optic Sensors," Proceedings of the NATO Advanced Study Institute on Optical Fiber Sensors, Kluwer Academic Publishers, Massachusetts, pp. 73-130, 1987.

[47] G. Beheim, J.L. Sotomayor, M.L. Tuma, and M. Tabib-Azar, "Fiber-Optic Temperature Sensor Using Laser Annealed Silicon Film," Integrated Optics and Microstructures II, Proc. SPIE, Vol. 2291, pp. 92-98, 1994.

[48] J.C. Hartle, E.W. Saaski, and G.L. Mitchell, "Fiber Optic Temperature Sensor using Spectral Modulation," Fiber Optic and Laser Sensors V, Proc. SPIE, Vol. 838, pp. 257-261, 1987.

[49] B. Hälg, "A Silicon Pressure Sensor with Low Cost Contactless Interferometer Optical Readout," Sensors and Actuators A, Vol. 30, pp. 225-230, 1992. 216-226, 1992.

[50] A. Méndez, T.F. Morse, and K.A. Ramsey, "Micromachined Fabry-Perot Interferometer with Corrugated Silicon Diaphragm for Fiber Optic Sensing Applications," Integrated Optics and Microstructures, Proc. SPIE, Vol. 1793, pp. 170-182, 1992.

[51] K. Fritsch and G. Beheim, "Wavelength-Division Multiplexed Digital Optical Position Transducer," Opt. Lett., Vol. 11, pp. 1-3, 1986.

[52] G.N. De Brabander, J.T. Boyd, G. Beheim, "Integrated Optical Ring Resonator With Micromechanical Diaphragm for Pressure Sensing," IEEE Photon. Tech. Lett., Vol. 6, No. 5, pp. 671-673, 1994.

[53] G.N. De Brabander, J.T. Boyd, G. Beheim, "Integrated Optical Interferometer with Micromechanical Diaphragm for Pressure Sensing," Integrated Optics and Microstructures II, Proc. SPIE, Vol. 2291, pp. 144-148, 1994.

[54] T. Bosselmann, P. Menke, "Intrinsic Temperature Compensation of Magnetooptic AC Current Transformers with Glass Ring Sensor Head," Proc. 10th Optical Fibre Sensors Conference, pp. 20-23, 1994.

[55] K. Kurosawa et. al., "Polarization Maintaining Properties of the Flint Glass Fiber for the Faraday Sensor Element," Proc. 10th Optical Fibre Sensors Conference, pp. 28-32, 1994.

[56] K.B. Rochford, A.H. Rose, M.N. Deeter, and G.W. Day, "Faraday Effect Current Sensor With Improved Sensitivity-Bandwidth Product," Proc. 10th Optical Fibre Sensors Conference, pp. 32-35, 1994.

[57] W. Lukosz, "Integrated Optical Nanomechanical Devices as Modulators, Switches and Tunable Filters, and as Acoustical Sensors," Integrated Optics and Microstructures, Proc. SPIE, Vol. 1793, pp. 214-234, 1992.

[58] S. Fujita, T. Kihara, M. Aoki, A. Hiroe, and K. Yokomori, "Integrated Waveguide Device for Magneto-Optical Disk Signal Detection and Its Fabrication Techniques," Miniature and Micro-Optics and Micromechanics, Proc. SPIE, Vol. 1992, pp. 140-149, 1993.

[59] M.J. Tudor, M.V. Andres, K.W.H. Foulds, and J.M. Naden, "Silicon Resonator Sensors: Interrogation Techniques and Characteristics," IEE Proc., Vol. 135, Pt. D, No. 5, pp. 364-368, 1988.

[60] S.D. Tilstra, "A Flourescence-Based Fiber Optic Temperature Sensor For Aerospace Applications," Specialty Fiber Optic Systems for Mobile Platforms, Proc. SPIE, Vol. 1589, pp. 32-37, 1991.

[61] V. Fernicola and L. Crovini, "A High Temperature Digital Fiber-Optic Thermometer," Proc. 10th Optical Fibre Sensors Conference, pp. 211-214, 1994.

[62] G. O'Keeffe et. al. "Development of an Intrinsic Phase Fluorimetric Oxygen Sensor Using a High Intensity Blue LED", Proc. 10th Optical Fibre Sensors Conference, pp. 461-464, 1994.

[63] A.J. Rogers,"Distributed Optical-Fibre Sensors, Proceedings of the NATO Advanced Study In Kluwer Academic Publishers, pp. 143-163, 1987.

[64] T.S.J. Lammerink, S.J. Gerritsen, "Fiber-Optic Sensors Based on Resonating Structures," Fiber Optic Sensors II, Proc. SPIE, Vol. 798, pp. 67-71, 1987.

[65] T. Nakayama, "Fiber LDA System," Proceedings of the NATO Advanced Study Institute on Kluwer Academic Publishers, pp. 217-226, 1987.

[66] H. Toda, M. Haruna, and H. Nishihara, "Optical Integrated Circuit for a Fiber Laser Doppler Velocimeter," J. Lightwave Tech., Vol. 5, No. 7, pp. 901-905, 1987.

[67] B. Culshaw, "Silicon in Optics," Fiber Optic Sensors II, Proc. SPIE, Vol. 798, pp. 346-353, 1987

[68] H. Uzeitig and H. Bartelt, "All-Optical Pressure Sensor with Temperature Compensation on Resonant PECVD Silicon Nitride Microstructures," Electron. Lett., Vol. 28, No. 4, pp. 40-402, 1992.

[69] Y.J. Rao and B. Culshaw, "Comparison Between Optically Excited Vibrations of Silicon Cantilever and Bridge Microresonators," Sensors and Actuators A, Vol. 30, pp. 203-208, 1992.

[70] M.V. Andres, M.J. Tudor, and K.W.H. Foulds, "Analysis of an Interferometric Optical Fiber Detecting Technique Applied to Silicon Vibration Sensors," ELectron. Lett., Vol. 23, pp. 774-775, 1987.

[71] R.E. Jones, J.M. Naden, R.C. Neat, "Optical-Fibre Sensors using Micromachined Silicon Resonant Elements," IEE Proc., Vol. 135, Pt. D, No. 5, pp. 353-358, 1988.

[72] D. Angelidis and P. Parsons, "Optical Micromachined Pressure Sensor for Aerospace Applications," Opt. Eng., Vol. 31, No. 8, pp. 1638-1641, 1992.

[73] K.E. Petersen, and C.R. Guarnieri, "Young's Modulus Measurements of Thin Film using Micromechanics," J. Appl. Phys., Vol. 50, pp. 6761-6766, 1979.

[74] Y. Uenishi, H. Tanaka, and H. Ukita, "AlGaAs/GaAs Micromachining for Monolithic Integration of Optical and Mechanical Components," Integrated Optics and Microstructures II, Proc. SPIE, Vol. 2291, pp. 82-91, 1994.

[75] Y.J. Rao and B. Culshaw, "Continuously Stable Selfoscillation of Silicon Cantilever Microresonators," Electron. Lett., Vol. 27, No. 19, pp. 1697-1699, 1991.

[76] S.C. Jensen, S.D. Tilstra, G.A.Barnabo, D.C. Thomas, and R.W. Philips, "A Fiber Optic Temperature Sensor for Aerospace Applications," Fiber Optic Systems for Mobile Platforms, Proc. SPIE, Vol. 1369, pp. 87-93, 1990.

REPORT DOCUMENTATION PAGE

Form Approved
OMB No. 0704-0188

1. AGENCY USE ONLY (*Leave blank*)	2. REPORT DATE	3. REPORT TYPE AND DATES COVERED
	May 1995	Technical Memorandum

4. TITLE AND SUBTITLE

"Fundamental Concepts" of Integrated and Fiber Optic Sensors

5. FUNDING NUMBERS

WU–505–62–50

6. AUTHOR(S)

Margaret L. Tuma

7. PERFORMING ORGANIZATION NAME(S) AND ADDRESS(ES)

National Aeronautics and Space Administration
Lewis Research Center
Cleveland, Ohio 44135–3191

8. PERFORMING ORGANIZATION REPORT NUMBER

E–9632

9. SPONSORING/MONITORING AGENCY NAME(S) AND ADDRESS(ES)

National Aeronautics and Space Administration
Washington, D.C. 20546–0001

10. SPONSORING/MONITORING AGENCY REPORT NUMBER

NASA TM–106920

11. SUPPLEMENTARY NOTES

Responsible person, Margaret L. Tuma, organization code 2540, (216) 433–8665.

12a. DISTRIBUTION/AVAILABILITY STATEMENT

Unclassified - Unlimited
Subject Category 74

This publication is available from the NASA Center for Aerospace Information, (301) 621–0390.

12b. DISTRIBUTION CODE

13. ABSTRACT *(Maximum 200 words)*

This chapter discusses fiber optic and integrated optic sensor concepts. Unfortunately, there is no standard method to categorize these sensor concepts. Here, fiber optic and integrated optic sensor concepts will be categorized by the primary modulation technique. These modulation techniques have been classified as: intensity, phase, wavelength, polarization, and time/frequency modulation. All modulate the output light with respect to changes in the physical or chemical property to be measured. Each primary modulation technique is then divided into fiber optic and integrated optic sections which are treated independently. For each sensor concept, possible sensor applications are discussed. The sensors and references discussed are not exhaustive, but sufficient to give the reader an overview of sensor concepts developed to date. Sensor multiplexing techniques such as wavelength division, time division, and frequency division will not be discussed as they are beyond the scope of this report.

14. SUBJECT TERMS

Fiber optic; Integrated optic; Sensor; Micromachining

15. NUMBER OF PAGES 37

16. PRICE CODE A03

17. SECURITY CLASSIFICATION OF REPORT	18. SECURITY CLASSIFICATION OF THIS PAGE	19. SECURITY CLASSIFICATION OF ABSTRACT	20. LIMITATION OF ABSTRACT
Unclassified	Unclassified	Unclassified	